

Defect energetics in MgO treated by first-principles methods

A. De Vita* and M. J. Gillan

Physics Department, University of Keele, Keele, Staffordshire ST5 5BG, United Kingdom

J. S. Lin,[†] M. C. Payne, and I. Štich[‡]

Cavendish Laboratory (TCM), University of Cambridge, Madingley Road, Cambridge CB3 0HE, United Kingdom

L. J. Clarke

Edinburgh Parallel Computer Centre, University of Edinburgh, Mayfield Road, Edinburgh EH9 3JZ, United Kingdom

(Received 17 April 1992)

Ab initio total-energy calculations have been performed on a parallel computer to study the formation and migration energies of cation and anion vacancies in MgO. The calculations are made in the framework of density functional and pseudopotential theory, using the supercell method, with the valence orbitals expanded in plane waves. The relaxed ground state is determined by conjugate-gradients minimization of the total-energy functional with respect to the plane-wave coefficients of occupied orbitals. The calculated defect energies are shown to be in remarkably close agreement with experiment and with values obtained from empirical modeling. We present results for the electron distribution surrounding the vacancies that show that the distortion induced in the oxygen ions is more complex than has previously been thought.

I. INTRODUCTION

The purpose of this paper is to report some of the first fully *ab initio* calculations of defect energetics in a ceramic oxide. Specifically, we have calculated the Schottky formation energy and the activation energies for cation and anion vacancy migration in MgO, using pseudopotential and density-functional methods. A preliminary brief account of this work has already appeared.¹

In the past, the treatment of the energetics of perfect and defective ionic materials has relied on empirical interaction models such as the shell model.²⁻⁴ While the empirical approach has achieved important successes, there is increasing recognition of the need for the more fundamental approach provided by *ab initio* methods. The direct first-principles treatment of defect energetics in an oxide such as MgO is, nevertheless, a major undertaking, and the present work has been made possible only by very recent advances in technique, and particularly by the exploitation of parallel methods. The substantial computational task needed was performed on a 64-node Meiko Computing Surface. More will be said below about the parallel computer code CETEP used in the work. We shall show that our calculated defect energies agree closely with available experimental values. The calculations also give important insight into the electronic structure of the defects, which we hope will open the way to improvements in the empirical modeling of materials such as MgO.

The methods we shall describe can be applied to a wide variety of materials. We have chosen to work on MgO for a number of reasons. First, oxides generally are rather difficult to model empirically, because of the large deformability of the O²⁻ ion, which is not a stable species in free space. *Ab initio* methods have an important role

to play in revealing the physics that should be incorporated in empirical models for such materials. Secondly, MgO has a wide-ranging importance as a high-temperature ceramic, a catalyst, and a mineral (it forms approximately 10% of the earth's lower mantle). Thirdly, MgO is the simplest representative of a large class of important oxides having the rocksalt structure.

There has already been a considerable amount of *ab initio* work on the energetics of ionic perfect crystals, much of it based on the Hartree-Fock approximation. (Perfect crystals are, of course, relatively straightforward to treat, because only calculations on small symmetrical unit cells are needed.) Particularly important has been the development of the Hartree-Fock code CRYSTAL,⁵ which has been used to study the electronic structure and energetics of a large number of ionic crystals.^{6,8} The pseudopotential density-functional techniques used in the present work have also been applied to perfect ionic crystals, including MgO, with excellent results.⁹⁻¹¹ Recently, a number of attempts have been made to use the Hartree-Fock approximation to study the energetics of ionic defects via calculations on clusters embedded in a representation of the bulk crystal. A recent example of this is the work of Grimes, Catlow, and Stoneham¹² on vacancies on MgO, which, though partially successful, was limited by the small size of clusters that could be handled, and by difficulties in achieving convergence with respect to the size of the basis set. Problems were also encountered in treating the positional relaxation of the ions—a very important effect for defects in ionic materials, because of the ionic polarization induced by the effective charge on the defect. It is also relevant to mention the work of Pisani *et al.*,¹³ which proposes a more sophisticated scheme for embedding the cluster in the surrounding crystal.

Our computational strategy is to perform all the calcu-

lations in periodic boundary conditions (sometimes known as the supercell method), with the electronic orbitals represented in a plane-wave basis. The pseudopotential treatment of materials containing first-row elements such as oxygen in a plane-wave basis requires carefully constructed "optimized" pseudopotentials,¹⁴ and even then large numbers of plane waves are needed. However, any such disadvantage is more than compensated by the major advantage of this approach, which is that the total energy can be systematically taken to complete convergence with respect to the size of the basis set. This is particularly important in treating charged defects, where the response of the electron distribution to the defect charge needs to be accurately described, and where we also need to be able to calculate the forces on the ion cores.

The calculation of defect energies, whether by the supercell method or otherwise, requires careful attention to the dependence of the results on the size of the system. What we are really aiming to calculate is the energies of isolated defects in an infinite crystal, so that we should, in principle, study the convergence of the energies with respect to cell size. This is a particular concern for charged defects treated by the supercell method, since one must consider the effect of Coulomb interactions between repeated images of the defects. Fortunately, these issues are already well understood from earlier work based on empirical modeling.^{15,16} However, in order to provide firm evidence for the case of MgO, we have supplemented our *ab initio* work with a set of calculations using an empirical interaction model, in which the vacancy energies are computed by the supercell method for a wide range of cell sizes. The results of these ancillary calculations, presented in the Appendix, indicate that sufficiently accurate results can be expected from systems of 32 ions, which is the size of the supercell used in our main *ab initio* calculations.

The theoretical and computational techniques used in this work are summarized in the following section; included in this section is an outline of the technique used to correct our Coulomb interactions between periodic defect images. Before attempting calculations on defects, we have made extensive calculations on the properties of the perfect crystal, the results of which have been checked against experiment and previous theoretical results; this part of the work is described in Sec. III. The defect calculations themselves are described in Sec. IV, where we also present results showing how the valence electrons are redistributed in response to the formation and migration of vacancies. The significance of our work, and the prospects for future calculations of the present kind on other oxides are discussed in Sec. V. Our supporting calculations based on an empirical model are reported in the Appendix.

II. THEORETICAL AND COMPUTATIONAL TECHNIQUES

We describe in this section first of all the general theoretical framework of the calculations, and then the issues involved in running them on a parallel machine. We also outline the considerations that arise in treating charged defects in periodic boundary conditions.

A. General framework

The calculations are based on the well-established methodology of density-functional theory in the local-density approximation (LDA), combined with the pseudopotential technique.¹⁷⁻¹⁹ The total ground-state energy of the system for any set of positions of the ion cores is found by determining the self-consistent orbitals of the valence electrons, with the interactions between these electrons and the magnesium and oxygen cores represented by *ab initio* nonlocal pseudopotentials. All the calculations are performed in periodic boundary conditions, using as a basis-set plane waves up to a chosen cutoff energy.

The pseudopotential method has long been in common use for nearly-free-electron materials such as aluminum and silicon, but has only begun to be used for materials containing first-row elements such as oxygen in the last few years. The difficulty for these elements comes from the fact that the valence $2p$ orbitals do not have core states of the same angular momentum lying below them, so that the cancellation theorem of pseudopotential theory does not apply.^{20,21} Consequently, the p -wave pseudopotential is strongly attractive, and the representation of the valence pseudo-wave-functions needs many plane waves. This problem has been mitigated by the recent development of "optimized" pseudopotentials.^{14,22} These are constructed as usual on the basis of all-electron atomic calculations, with the condition of norm conservation,²³ but with the additional requirement that the kinetic energy associated with each pseudoorbital above a chosen wave vector be minimized. A further key element in the present work is that the Kleinman-Bylander representation of the pseudopotentials is used.^{11,24} This allows the plane-wave matrix elements of the pseudopotentials to be expressed in separable form, a feature which is essential for calculations on the large systems needed in the present work.

The oxygen pseudopotential we use has the optimized form, with an optimization wave vector for the p wave equal to 5.7 a.u. The reference atomic configurations used to construct it were $2s^2 2p^4$ for the s and p components, and $2s^2 2p^{2.5} 3d^{0.5}$ for the d component, with real-space cutoffs for these three components equal to 1.25, 1.25, and 1.45 a.u. The d -wave component was taken to be the local part of the Kleinman-Bylander representation. Optimization is not needed for magnesium, and we have used the standard Kerker method of pseudopotential generation,²⁵ with reference atomic configurations of $3s^2$ for the s component, and $3s^{0.5} 3p^{0.25} 3d^{0.25}$ for p and d components, and real-space cutoffs of 1.38, 1.98, and 2.03 a.u. In this case, the s -wave component has been treated as local. Both pseudopotentials have been shown to be highly transferable over the required energy ranges, and to be free of the "ghosts" which can sometimes afflict the Kleinman-Bylander form.²⁶

The computational strategy of the calculations incorporates two key ideas of the Car-Parrinello method.²⁷ First, the ground state is determined by global minimization of the energy functional with respect to the plane-wave coefficients of all the occupied orbitals (rather than,

for example, by repeated diagonalization of the Kohn-Sham Hamiltonian). This is essential for the very large plane-wave basis sets and numbers of occupied orbitals we have to treat. The minimization is performed by the preconditioned conjugate-gradients technique developed by Teter *et al.*²⁸ Important features of the method are that the orbital coefficients are updated in a band-by-band manner, which allows a substantial saving of memory compared with other methods (e.g., Ref. 29), and that variation of the Kohn-Sham Hamiltonian during the minimization search is fully included, which avoids the problem of "charge sloshing."²⁸ A second, unrelated, concept borrowed from the Car-Parrinello method is that of repeated transformation of orbitals from real to reciprocal space and back. This exploits the fact that the kinetic-energy operator is diagonal in reciprocal space and most of the potential energy operator is diagonal in real space. (A very recent advance not included in the present work is the treatment of the Kleinman-Bylander nonlocal potential in real space.³⁰) Because of these repeated transformations, the calculations rely heavily on efficient fast-Fourier methods.

Other, more minor, points of technique are as follows. First, we note that in the Mg atom there is an appreciable overlap between the 3s and 2p orbitals, which means that the nonlinear core correction of Louie, Froyen, and Cohen³¹ may be significant; we return to this question later in the paper. Second, Brillouin-zone sampling is essential, even for the 32-ion systems we use; we have used the standard Monkhorst-Pack scheme.³² Third, the exchange-correlation energy is represented by the usual Perdew-Zunger form,³³ though we shall mention the effects of using other forms.

B. The parallel code

Only very brief details of the parallel code CETEP (Cambridge-Edinburgh total-energy package) are given here, since a full description will be published elsewhere.³⁴ In designing a parallel code for total-energy calculations, the most important issue is the strategy to be followed in distributing the computation between processors. After considering a number of strategies, we have concluded that for the parallel machines available to us at present the optimal method is to parallelize over regions of real or reciprocal space. This exploits the fact that most of the terms in the total-energy functional are diagonal in either real or reciprocal space. Real space (or reciprocal space) is divided into disjoint regions assigned to different processors, which work independently on the calculation of quantities in these regions. When performing fast-Fourier transforms between the two spaces, the data need to be redistributed between processors. The requirement that the amount of such redistribution be kept to a minimum is one of the main factors in deciding how to assign regions to processors. In our implementation, each processor is in charge of either a set of planes on the real-space grid or a set of columns on the reciprocal-space grid, depending on the part of the calculation involved. The efficiency of the calculations is enhanced by assembly coding of the one-dimensional fast-Fourier calculations which make up the three-dimensional trans-

form, and by specially written communication routines for the redistribution of data across processors. Full details, and results on the timing and performance of the code are given by Clarke, Štich, and Payne.³⁴

C. Charged defects in repeated geometry

The main focus of this work is on the energetics of isolated vacancy defects. We perform the calculations in periodic boundary conditions by having a single vacancy in each repeated cell. Vacancies in MgO carry a net charge: a Mg vacancy is formed by removal of a Mg core without changing the number of valence electrons, while an O vacancy is formed by removing an O core together with eight valence electrons; the net charges of the Mg and O vacancies are thus $-2e$ and $2e$, respectively. (We note that other charge states are also possible; for example, under suitable conditions, *F* centers consisting of an electron bound to an oxygen vacancy can be formed. These, however, are not of interest here. We are also not concerned in the present work with the unoccupied acceptor and donor levels associated with the vacancies, although these are clearly of great interest. Our sole concern here is with ground-state energetics.) Because of the net charges carried by the defects, the sum of the core and electron charges in each supercell is not zero when a vacancy is present. This gives rise to two questions: first, how to ensure that the total energy per supercell makes mathematical sense; second, how to correct for the interaction of the vacancies with each other's polarization fields.

These issues are not peculiar to *ab initio* calculations. They arise in exactly the same form in the treatment of charged defects with empirical interaction models. It is well established¹⁵ that charged defects can be treated in periodic boundary conditions, provided we suppose the net charge of cores and electrons to be compensated by a uniform background. The residual Coulombic interaction between defects can be derived by a simple physical argument.¹⁵ According to this, the leading contribution to the interaction energy per defect ΔE can be obtained by regarding the defects as point charges in a uniform dielectric, so that it is given by

$$\Delta E = -\frac{1}{2}\alpha q^2/\epsilon_0 L, \quad (1)$$

where q is the net defect charge, ϵ_0 is the static dielectric constant of the bulk crystal, L is the lattice parameter of the supercell, and α is the appropriately defined Madelung constant. When the defect formation energy is obtained by subtracting the energy of the perfect system from that of the defective system, the correction ΔE is subtracted from the result to obtain an improved value.

In order to demonstrate the correctness of this procedure, we report in the Appendix calculations on vacancies in MgO performed in periodic boundary conditions with a well-established empirical interaction model. The calculations demonstrate that the formation energies calculated in this way converge rapidly with increasing supercell size, and that they converge to the values obtained by applying the more conventional Mott-Littleton method^{2,3,35} to the same interaction model. Migration

energies are also shown there to converge rapidly. This provides the justification for the extraction of formation and migration energies from *ab initio* calculations on 32-ion systems reported later in the paper.

III. THE PERFECT CRYSTAL

Before attempting calculations on defects, we have made extensive tests of our computational methods on the MgO perfect crystal. By making calculations on the two-ion primitive cell, we have studied the influence of the plane-wave cutoff, the number of Brillouin-zone sampling points, the nonlinear core correction, and the choice of exchange-correlation function.

Our tests on the plane-wave cutoff were made using four Monkhorst-Pack sampling points, i.e., with the scheme $q=2$ in the notation of Monkhorst and Pack.³² Our results show that the total energy converges very rapidly for cutoffs above 600 eV. For a cutoff of 1000 eV, the total energy per unit cell is converged to within better than 0.05 eV (i.e., 0.01% of the total energy), and all our remaining calculations on the perfect crystal have been performed with this cutoff. As we show below, a smaller cutoff can be used when calculating energy differences.

In testing the convergence with respect to sampling, we bear in mind that our main interest is in large systems containing 16 or 32 ions. We wish to know how many Monkhorst-Pack points are needed for these systems. Provided we restrict ourselves to the perfect crystal, questions like this can be answered without doing calculations on large systems. For example, a calculation on a 32-ion repeating cell of perfect crystal is precisely equivalent to a calculation on the 2-ion unit cell performed with an appropriately chosen "folded-out" sampling set. Our tests show that Γ -point sampling is not really adequate even for the 32-ion system, but that the four-point set should be extremely accurate for the 16- and 32-ion systems, giving an error of less than 0.01 eV in the total energy per cell. However, for calculations on the distorted 2-ion perfect crystal needed to obtain the transverse-optic frequency (see below), the four-point set is not adequate, and we have used 16 sampling points in this case.

The core correction due to the nonlinear dependence of the exchange-correlation energy on electron density produces important effects if there is a significant overlap between core and valence wave functions.³¹ The overlap is negligible for oxygen, but the slight overlap for the magnesium atom (Fig. 1) makes the correction worth investigating. We have implemented the correction using the standard procedure described by Louie, Froyen, and Cohen.³¹ Its effects turn out to be small, but will be noted below where appropriate.

Our calculated values of the equilibrium lattice parameter a_0 , the bulk modulus, the zone-center transverse-optic frequency, and the four phonon frequencies at the X point for this value of a_0 are listed in Table I. The reported value of lattice parameter does not include the core correction, which reduces it by 0.5%. This variation is well within the uncertainty from other sources. For comparison, the use of the Wigner form for exchange correlation,⁴⁰ instead of the Perdew-Zunger form used

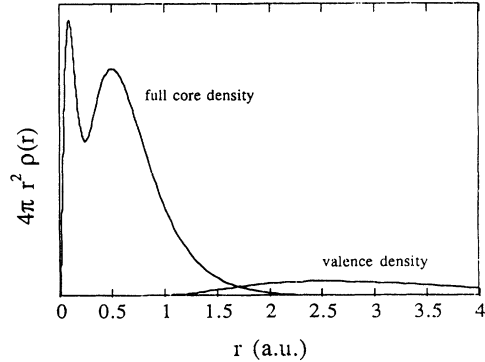


FIG. 1. Contributions to the electron density $\rho(r)$ as a function of radial distance r due to core electrons and valence electrons in the neutral Mg atom, showing the slight overlap in the region 1.5–2.0 a.u. The densities are calculated in the local density approximation, using the Perdew-Zunger form for exchange and correlation.

here, increases the lattice parameter by 0.9%. However, the core correction is included in the TO frequency, which is the one case where it is significant. Without the correction, the frequency is lower by 0.8 THz. The excellent agreement with experiment for all quantities confirms that technical aspects of the calculations are under adequate control.

To provide a reference point for the results of the following section, we show in Fig. 2 our calculated density distribution of valence electrons in the perfect crystal. The strongly ionic nature of MgO, which is well known from other calculations based on both the Hartree-Fock and pseudopotential-LDA methods,¹⁰ is very clear from the figure. The valence charge is almost entirely localized on the oxygen ions, so that the magnesium ions are completely invisible. We hope to report elsewhere on the detailed comparison between the present results for the density distribution and those produced by Hartree-Fock calculations.

TABLE I. Calculated and experimental values of lattice parameter a_0 , bulk modulus B , and five phonon frequencies of MgO. Phonon modes are the transverse-optic mode at the Γ point and the transverse and longitudinal-acoustic and -optic modes at the X point of the Brillouin zone.

	Calculated	Experimental
a_0 (Å)	4.17	4.21 ^a
B (Mbar)	1.54	1.55 ^b –1.62 ^c
TO(Γ) (THz)	12.39	12.23 ^d
TA(X) (THz)	8.65	8.96 ^b
LA(X) (THz)	12.57	12.65 ^b
TO(X) (THz)	13.24	13.15 ^b
LO(X) (THz)	16.36	16.61 ^b

^aWyckoff (Ref. 26).

^bSangster, Peckham, and Saunderson (Ref. 37).

^cAnderson and Andreatch (Ref. 38).

^dJasperse *et al.* (Ref. 39).

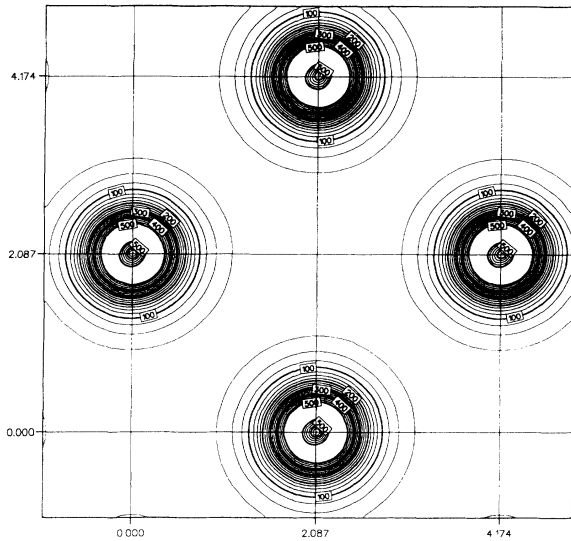


FIG. 2. Contour plot of the calculated valence electron density (units of 10^{-2} \AA^{-3}) on the (100) plane in perfect-crystal MgO. The contours are uniformly spaced at intervals of $25 \times 10^{-2} \text{ \AA}^{-3}$. Intersections of the grid lines mark regular-lattice sites. Distance along the edge of the plot is indicated in angstrom units.

IV. DEFECT ENERGETICS

A. The Schottky formation energy

The Schottky energy E_S is the sum of the energies needed to extract a Mg^{2+} ion and an O^{2-} ion to form isolated relaxed Mg and O vacancies, minus the cohesive energy per ion pair. For a given size of cell, we therefore need the energies of (i) the perfect crystal; (ii) the system formed from (i) by extracting a Mg core; (iii) the system formed from (i) by extracting an O core and eight electrons. The quantity E_S is obtained as the small difference between large energies and it is essential that the same plane-wave cutoff and sampling vectors be used in calculating these three energies. Our calculations of E_S have been performed for supercells containing 16 and 32 ions, using four sampling points. For the 16-ion system, we use a cutoff of 1000 eV. The 32-ion calculations employ a cutoff of 600 eV, which corresponds to a basis set of about 15 000 plane waves. The justification for using this cutoff, which is somewhat lower than what we used for the perfect-lattice properties, comes from tests performed on the unrelaxed vacancy formation energy in the eight-ion system. Calculations on this system show that reduction of the cutoff energy from 1000 to 600 eV changes the Schottky energy by less than 0.05 eV, even though the absolute total energies are less completely converged.

Relaxation of the ionic positions in the vacancy systems is, of course, crucial, because the relaxation energies are substantial. In the 16-site system, this poses no problem since the cubic symmetry of the vacancy leaves only a single positional degree of freedom, namely, the radial distance of the ion immediately next to the vacancy. Here, the relaxed geometry was determined from the to-

tal energy of the system for a series of values of the relaxation coordinate. In the 32-site vacancy systems, where there are many more degrees of freedom, we have made use of our calculations based on the empirical interaction model⁴¹ reported in the Appendix. The relaxed ionic positions given by this model in the same supercell geometry turn out to be close to the relaxed *ab initio* positions; this can be established from the magnitudes of the residual forces acting on the ion cores. We therefore get accurate enough results for the relaxed total energy if we use the empirically calculated relaxed positions in the *ab initio* calculations. When this is done, the residual forces on the ions are less than, and for most of the ions much less than, 0.4 eV/Å; from this, we can show that further relaxation would lower the total energy by no more than 0.1 eV, which is not significant.

We report in Table II the unrelaxed and relaxed

TABLE II. *Ab initio* total energies of the periodic systems used to study the energetics of defective MgO, together with the resulting Schottky energy E_S and cation and anion migration energies ΔE_m compared with values from experiment and from empirical modeling. *Ab initio* results are shown for 16-ion and 32-ion supercells, with the individual energies numbered to allow the relations between them to be indicated. The correction referred to in items (6) and (10) is the Madelung term given in Eq. (1).

	16 ions	32 ions
(1) Perfect lattice (total)	-3711.197	-7384.963
(2) Perfect lattice (per unit cell)	-463.900	-461.560
(3) Mg vacancy (unrelaxed)	-3667.749	-7339.924
(4) Mg vacancy (relaxed)	-3668.136	-7341.224
Mg extraction energy:		
(5) Uncorrected (4)-(1)	43.061	43.739
(6) Corrected	44.633	44.987
(7) O vacancy (unrelaxed)	-3284.272	-6961.171
(8) O vacancy (relaxed)	-3285.718	-6962.754
O extraction energy:		
(9) Uncorrected (8)-(1)	425.479	422.209
(10) Corrected	427.051	423.457
Schottky energy:		
(11) <i>Ab initio</i> (6)+(10)-(2)	7.784	6.884
(12) Experimental		4-7 ^a
(13) Empirical model		7.72 ^b
(14) Migrating Mg vacancy		-7338.831
(15) Migrating O vacancy		-6960.273
Mg migration energy:		
(16) <i>Ab initio</i> (14)-(4)		2.393
(17) Experimental		2.2, ^c 2.28 ^d
(18) Empirical model		2.07 ^b
O migration energy		
(19) <i>Ab initio</i> (15)-(8)		2.481
(20) Experimental		2.42, ^e 2.61 ^f
(21) Empirical model		2.11 ^b

^aMackrodt (Ref. 43).

^bSangster and Rowell (Ref. 44).

^cDuclot and Departes (Ref. 45).

^dSempolinski and Kingery (Ref. 46).

^eShirasaki and Harma (Ref. 47).

^fShirasaki and Yamamura (Ref. 48).

ground-state energies of the 16- and 32-site systems containing either a Mg or an O vacancy, together with the energies of the corresponding perfect crystals obtained with the same cutoff and sampling set. The Mg and O extraction energies obtained from these numbers are corrected for the Coulomb interaction between periodic images, as described in Sec. II C. The static dielectric constant ϵ_0 entering this correction is taken to have its experimental value of 9.86.⁴² The uncorrected and corrected extraction energies for the relaxed vacancies, together with the resulting values of the Schottky formation energy are given in Table II.

For both sizes of repeating cell, the calculated Schottky energy is approximately 7 eV which is remarkably close to the predictions from empirical modeling, which are also included in Table II. In judging the degree of convergence with respect to cell size, reference should be made to the results of calculations using an empirical potential reported in the Appendix. These suggest that further increase of cell size is unlikely to change the results by more than a few tenths of an eV. The relation with experimental results will be discussed in Sec. V.

Because the defects carry net charges, we expect them to induce a strong polarization of the surrounding lattice, and to distort the electron clouds on neighboring ions. The response of the electron density to the formation of vacancies is conveniently studied by subtracting the electron density in the perfect crystal from that in the vacancy system. To make this meaningful, we do this using the electron density in the *unrelaxed* vacancy system, because otherwise the difference arising simply from the displacement of the ions would confuse the issue. Contour plots of this difference density on the (100) and (110) planes for the Mg and O vacancies are displayed in Figs. 3 and 4. As for the perfect crystal (Fig. 2), the Mg ions are almost invisible on these plots, since the electron density in their vicinity is so small.

In both plots, the prominent features represent the distortion of charge density on the neighboring oxygen ions, which is considerably more complex than would be predicted by empirical models such as the shell model.^{3,41,43} For the Mg vacancy, the valence electrons on neighboring oxygens are repelled by the effective negative charge of the vacancy. The figure shows that the charge redistribution is due mainly to the distortion of the oxygen *p* orbitals pointing towards the vacancy. The double peak-trough structure arises from the shift of charge within the lobes of these orbitals. For the oxygen vacancy, the main consequence of the effective positive charge on the defect is seen to be not the polarization of the nearest oxygens but the transfer of electrons from these neighbors to a spherical shell region embracing the Mg neighbors of the vacancy. The transfer is mainly from the *p* orbitals pointing towards the vacancy, and this leaves a prominent quadrupole moment on the oxygen neighbors.

B. The vacancy migration energies

The vacancy migration energy for each type of vacancy is obtained from a calculation of the relaxed ground-state energy when the migrating ion is constrained to lie midway between two neighboring half-vacancies on the ap-

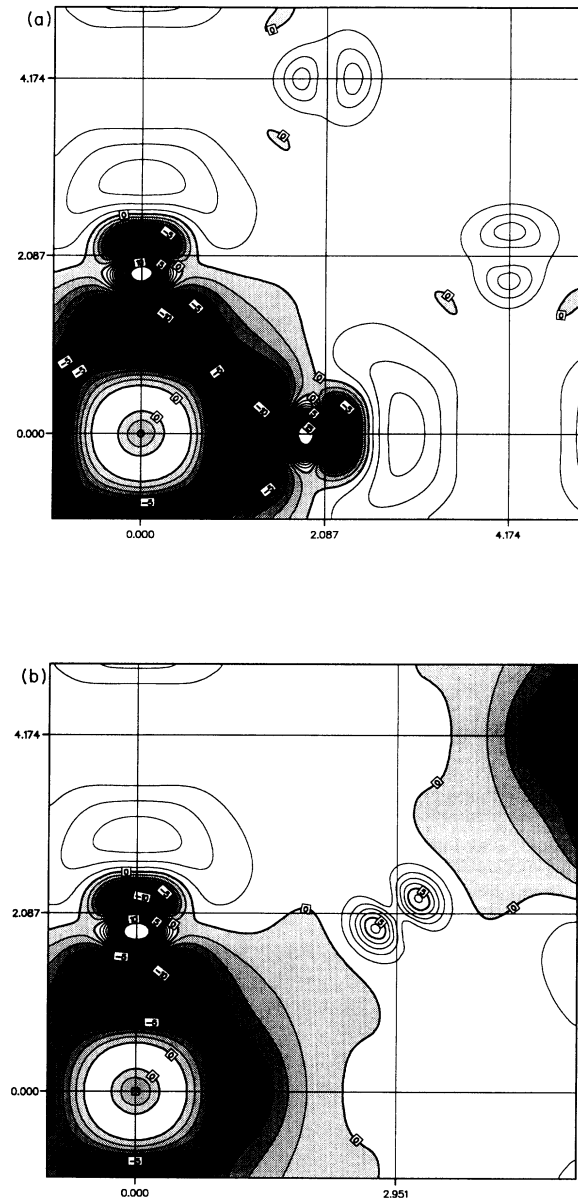


FIG. 3. Difference valence density (defective system minus perfect crystal) for the Mg^{2+} vacancy in MgO on (a) the (100) plane and (b) the (110) plane. Density is in units of 10^{-2} \AA^{-3} , with contours at intervals of 10^{-2} \AA^{-3} , and negative regions shown shaded. Intersections of the grid lines mark regular-lattice sites, with the vacancy site at the origin of coordinates. Distance along the edge of the plot is indicated in angstrom units.

propriate sublattice. These calculations have been performed only on the 32-site system since empirical calculations (see Appendix) indicate that the 16-site system would be too small. As for the formation energy calculations on the 32-site system, an explicit relaxation of ionic positions has not been performed. Instead a good estimate of the relaxed positions is obtained from the empirical calculations. The residual forces on the ions in the self-consistent ground states give a guide to the addition-

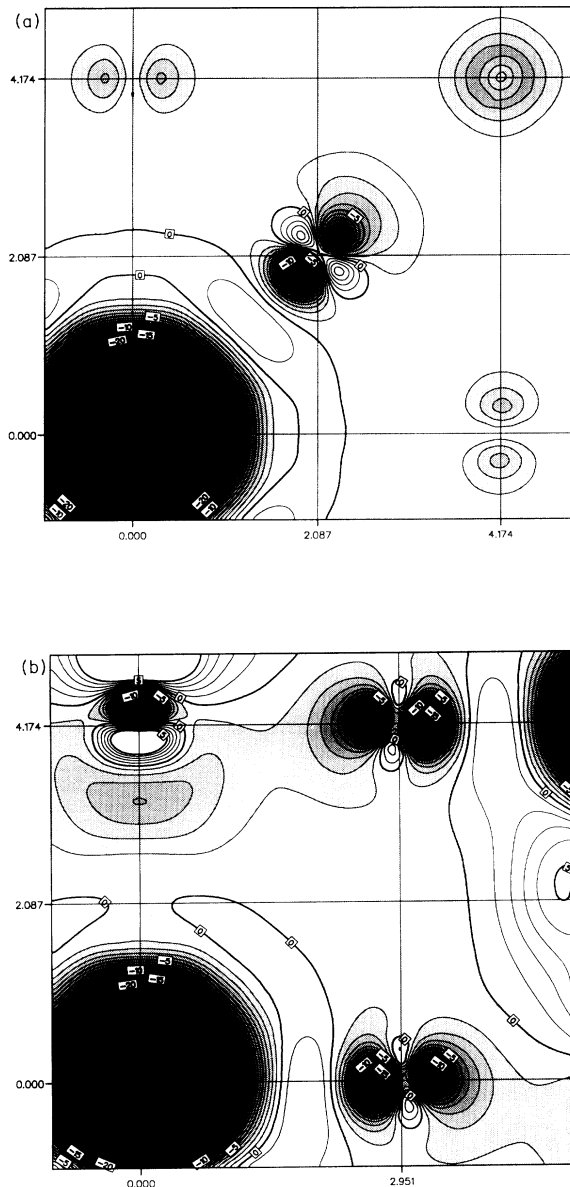


FIG. 4. Difference valence density (defective system minus perfect crystal) for the O^{2-} vacancy in MgO on (a) the (100) plane and (b) the (110) plane. Other details are the same as for Fig. 3.

al relaxation energy remaining, and allow us to conclude that this is less than 0.1 eV. The Madelung correction is, of course, independent of the vacancy position, so that the migration energy is obtained by subtracting the uncorrected energy of the relaxed equilibrium vacancy system from the uncorrected energy of the relaxed migrating vacancy system.

Table II gives our *ab initio* migration energies, compared with the results of empirical modeling and experimental values. The agreement between *ab initio* calculation and experiment is remarkable, the discrepancies for both vacancies being no more than 0.2 eV. Contour plots of the valence electron density for the saddlepoint

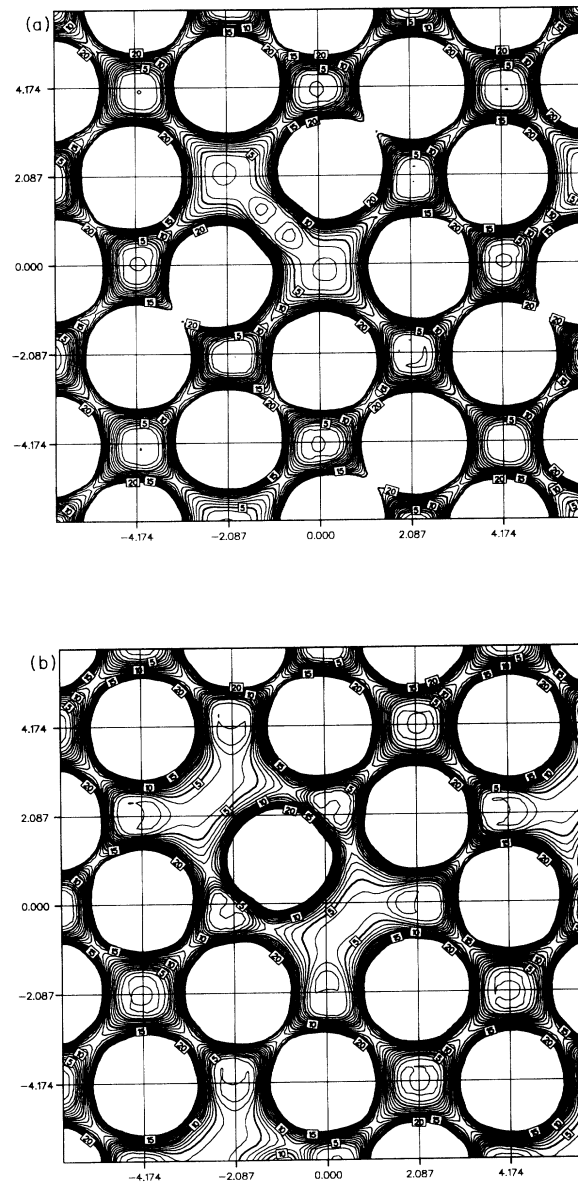


FIG. 5. Total valence electron density on the (100) plane for (a) the migrating Mg^{2+} vacancy and (b) the migrating O^{2-} vacancy. In both cases, the system is fully relaxed, with the migrating ion held at the saddle point, midway between initial and final sites. Units of density are 10^{-2} \AA^{-3} , with contours at intervals of 10^{-2} \AA^{-3} . The plots are cut off for densities above $20 \times 10^{-2} \text{ \AA}^{-3}$. Distance along the edge of the plot is indicated in angstrom units.

configuration of the migrating vacancies are shown in Fig. 5.

V. DISCUSSION

One of the main objectives of this work has been to demonstrate the feasibility of calculating the energetics of defects in ionic oxides such as MgO entirely from first principles. In order to achieve this objective, it has been essential to work with large systems, and at the same time

to ensure complete convergence with respect to the size of the basis set by using a sufficiently large cutoff energy. Calculations of this kind are computationally extremely demanding. The availability of a highly parallel computer, and the development of the parallel computer code CETEP described in Sec. II B were crucial to the success of the project. However, we stress our belief that the current rapid progress in parallel technology will make calculations of the kind we have described routinely available within a few years. Even with the 64-node Meiko Computing Surface being used in this project, substantial improvements already achieved in the coding of CETEP will enable considerably more ambitious calculations to be undertaken very soon.

Larger calculations are desirable. We have paid close attention in this work to the convergence of the defect energies with respect to the size of repeated system, and we have sought to buttress our methods by making use of comparisons with empirical modeling results. We have argued from these comparisons that our *ab initio* results for the Schottky and migration energies are probably within a few tenths of an eV of the limiting values for completely isolated defects, which is certainly accurate enough for practical purposes. It is still true, however, that the results would be further strengthened by calculations on larger systems. It would also be an advantage to be able to relax the ionic positions without appealing, as we have chosen to do here, to empirical modeling. Progress in both these areas is expected very shortly.

The comparisons with experiment that we have been able to make fully confirm the reliability of our calculations. At present, the experimental situation is satisfactory only for the migration energies of the cation and anion vacancies, where there is close agreement between different experimental measurements. Our *ab initio* results reproduce these migration energies with remarkable accuracy, the discrepancies of ~ 0.1 eV being comparable with the spread of experimental values. The striking similarity of the migration energies for cation and anion vacancies, also predicted by the empirical interaction models, is fully confirmed by our results. Unfortunately, because the Schottky formation energy E_S is so large, the concentration of intrinsic defects is minute even near the melting point, and E_S is therefore very difficult to measure experimentally. Measured values lie in the range 4–7 eV (see Ref. 43). Given this large uncertainty, it has been necessary up to now to rely on the predictions of empirical models. The close agreement of our *ab initio* value for E_S with the empirical predictions is therefore important, because it confirms the reliability of empirical modeling for this quantity. There are many other cases where defect formation energies in oxides are difficult to measure (see, e.g., Ref. 49), and we believe that the present kind of *ab initio* calculation has much to offer in this area.

An important assumption of the shell-model description is that electron redistribution consists only of an effective displacement of the valence charge relative to the core charge on each ion. *Ab initio* calculations on defects are important because they allow us to study the true charge redistribution in detail. The results we have

presented give only preliminary glimpses into this matter. However, we have shown that the redistribution induced by both the Mg and O vacancies is more complicated than would be suggested by the shell model. This is particularly true of the O vacancy, where charge transfer and quadrupolar distortion effects are clearly visible. How these unexpected effects can be reconciled with the apparent correctness of shell-model energetics will be an important matter for future study.

Encouraged by the results of the present work, we are now exploring the capabilities of the present techniques by applying them to a series of other oxides. Calculations on the energetics of Li Frenkel defects in Li_2O have already been completed and will be reported soon. Work on the bulk, defect, and surface properties surface of $\alpha\text{-Al}_2\text{O}_3$ (corundum) is also under way.

ACKNOWLEDGMENTS

The calculations reported here were performed as part of the "Grand Challenge" collaborative project on a 64-node Meiko Computing Surface at Edinburgh University. We are grateful to the SERC for the funding which supports the work. We have received support from a number of people at Edinburgh University, notably Professor D. Wallace, Dr. K. Bowler, and Dr. S. Booth. Other members of the Grand Challenge team who have greatly assisted us are Dr. D. Bird and Dr. G. Ackland. R. Ferneyhough provided valuable assistance in the production of the graphics. L.J.C. acknowledges funding received under a SERC contract, and J.S.L. thanks Dr. N. Troullier for stimulating discussions. The work of A.D.V. was supported by a SERC grant.

APPENDIX: EMPIRICAL MODELING WITH PERIODIC BOUNDARIES

We present here some results for the energetics of vacancies in MgO calculated using an empirical interaction model in periodic boundary conditions. The aim of these ancillary calculations is to give insight into the size of system needed to obtain reliable results. In the *ab initio* work presented in this paper, our aim is to obtain reliable values for the formation and migration energies of isolated defects. In order to do this with confidence, we need some idea of the way the calculated defect energies converge as the size of the supercell tends to infinity. This cannot yet be explicitly examined in the *ab initio* calculations, but it can be rather easily studied with empirical models. In addition, the empirical results obtained in periodic boundary conditions can be directly checked against values obtained from the same empirical model with the Mott-Littleton method.^{2,3,35} In this method, the defect is directly treated in the infinite crystal, with a set of ions in its immediate neighborhood handled explicitly, and the remainder of the crystal treated as a dielectric continuum.

In appealing to empirical modeling in this way, we are making the reasonable assumption that the asymptotic dependence of the energies on supercell size will be qualitatively the same in *ab initio* and empirical treatments.

TABLE III. Values for the Schottky energy E_S and the cation and anion migration energies ΔE_m in MgO calculated in periodic boundary conditions using the empirical shell-model potential of Sangster and Stoneham (Ref. 41). Results are shown for a range of different sizes of supercells, and include the Madelung correction [see Eq. (1)]. Also shown are the defect energies calculated from the same interaction model for the infinite crystal using the Mott-Littleton method [Sangster and Rowell (Ref. 44)].

No. of ions	E_S (eV)	ΔE_m (eV)	
		Cation	Anion
16	7.03	1.58	1.53
32	7.03	2.36	2.48
54	7.41	2.15	2.23
64	7.34	2.22	2.32
128	7.55	2.11	2.21
250	7.60	2.08	2.19
432	7.63		
Mott-Littleton	7.72	2.07	2.11

We have chosen to use the well-established interaction model of Sangster and Stoneham,⁴¹ which is a shell model in which the Mg and O ions have full ionic charges of $2e$ and $-2e$, and interact via potentials of the standard

Born-Mayer-Huggins form. The supercell calculations were performed using the computer code SYMLAT.⁵⁰ Since the computations are rapid, it is not difficult to treat systems containing several hundred ions.

Table III shows results for the empirically calculated Schottky energy, including the Madelung correction described in Sec. II C, and the cation and anion vacancy migration energies, for sizes of supercells going up to over 400 ions. For comparison, we also quote results from the same interaction model obtained by the Mott-Littleton method.⁴⁴ A number of conclusions are clear. First, the supercell values for all the defect energies converge quite rapidly with increasing cell size to the Mott-Littleton (infinite-crystal) values. Second, with the supercell size of 32 ions, the residual error in the Schottky energy E_S is about 0.6 eV, or somewhat less than 10%. This accuracy is already extremely useful. It suggests, though, that it would be desirable in the *ab initio* work to go to systems of 54 and 64 ions, which would substantially reduce the error. Third, the migration energies are already rather well converged for systems of 32 ions, the absolute errors being about 0.3 eV. Again, the ability to go to the next size of the supercell would give worthwhile improvements. Enhancements in the coding of CETEP will make *ab initio* calculations on these larger systems feasible in the near future.

*Also at Istituto di Chimica Applicata ed Industriale, via A. Valerio 2, 34127 Trieste, Italy.

†Present address: The Royal Institution, 21 Albemarle Street, London W1X 4BS, United Kingdom.

‡Also at Institute of Inorganic Chemistry, Slovak Academy of Sciences, CS-842 36 Bratislava 43, Czechoslovakia.

¹A. De Vita, M. J. Gillan, J. S. Lin, M. C. Payne, I. Štich, and L. J. Clarke, Phys. Rev. Lett. **68**, 3319 (1992).

²N. F. Mott and M. J. Littleton, Trans. Faraday Soc. **34**, 485 (1938).

³Computer Simulation of Solids, edited by C. R. A. Catlow and W. C. Mackrodt (Springer-Verlag, Berlin, 1982).

⁴J. H. Harding, Rep. Prog. Phys. **53**, 1403 (1990).

⁵R. Dovesi, C. Pisani, C. Roetti, and V. R. Saunders, Phys. Rev. B **28**, 5781 (1983).

⁶R. Dovesi, C. Ermondi, E. Ferrero, C. Pisani, and C. Roetti, Phys. Rev. B **29**, 3591 (1984).

⁷M. Causà, R. Dovesi, C. Pisani, and C. Roetti, Phys. Rev. B **33**, 1308 (1986).

⁸R. Nada, C. R. A. Catlow, R. Dovesi, and C. Pisani, Phys. Chem. Min. **17**, 353 (1990).

⁹S. Froyen and M. L. Cohen, Phys. Rev. B **29**, 3770 (1984).

¹⁰K. J. Chang and M. L. Cohen, Phys. Rev. B **30**, 4774 (1984).

¹¹D. C. Allan and M. P. Teter, Phys. Rev. Lett. **59**, 1136 (1987).

¹²R. W. Grimes, C. R. A. Catlow, and A. M. Stoneham, J. Phys. Condens. Matter **1**, 7367 (1989).

¹³C. Pisani, R. Dovesi, R. Nada, and L. N. Kantorovich, J. Chem. Phys. **92**, 7448 (1990).

¹⁴A. M. Rappe, K. M. Rabe, E. Kaxiras, and J. D. Joannopoulos, Phys. Rev. B **41**, 1227 (1990).

¹⁵M. Leslie and M. J. Gillan, J. Phys. C **18**, 973 (1985).

¹⁶N. L. Allan, W. C. Mackrodt, and M. Leslie, Adv. Ceram. **23**, 257 (1987).

¹⁷G. P. Srivastava and D. Weaire, Adv. Phys. **36**, 463 (1987).

¹⁸J. Ihm, Rep. Prog. Phys. **51**, 105 (1988).

¹⁹M. J. Gillan, in Computer Simulation in Materials Science, Vol. 205 of NATO Advanced Study Institute, Series E: Applied Science, edited by M. Mayer and V. Pontikis (Kluwer, Dordrecht, 1991), p. 257.

²⁰V. Heine, in Solid State Physics, edited by H. Ehrenreich, F. Seitz, and D. Turnbull (Academic, New York, 1970), Vol. 24, p. 1

²¹M. L. Cohen and V. Heine, in Solid State Physics (Ref. 20), p. 37.

²²J.-S. Lin, A. Qteish, M. C. Payne, and V. Heine (unpublished).

²³D. R. Hamann, M. Schlüter, and C. Chiang, Phys. Rev. Lett. **43**, 1494 (1979).

²⁴L. Kleinman and D. M. Bylander, Phys. Rev. Lett. **48**, 1425 (1980).

²⁵G. P. Kerker, J. Phys. C **13**, L189 (1980).

²⁶X. Gonze, P. Käckell, and M. Scheffler, Phys. Rev. B **41**, 12 264 (1990).

²⁷R. Car and M. Parrinello, Phys. Rev. Lett. **55**, 2471 (1985).

²⁸M. P. Teter, M. C. Payne, and D. C. Allan, Phys. Rev. B **40**, 12 255 (1989).

²⁹M. J. Gillan, J. Phys. Condens. Matter **1**, 689 (1989).

³⁰R. D. King-Smith, M. C. Payne, and J.-S. Lin, Phys. Rev. B **44**, 13 063 (1991).

³¹S. G. Louie, S. Froyen, and M. L. Cohen, Phys. Rev. B **26**, 1738 (1982).

³²H. J. Monkhorst and J. D. Pack, Phys. Rev. B **13**, 5188 (1976).

³³J. Perdew and A. Zunger, Phys. Rev. B **23**, 5048 (1981).

³⁴L. J. Clarke, L. Štich, and M. C. Payne (unpublished).

³⁵A. B. Lidiard and M. J. Norgett, in Computational Solid State Physics, edited by F. Herman, N. W. Dalton, and T. R. Koehler (Plenum, New York, 1972).

- ³⁶R. W. G. Wyckoff, *Crystal Structures* (Wiley, New York, 1963).
- ³⁷M. J. L. Sangster, G. Peckham, and D. H. Saunderson, *J. Phys. C* **3**, 1026 (1970).
- ³⁸O. L. Anderson and P. Andreatch, *J. Am. Ceram. Soc.* **49**, 404 (1966).
- ³⁹J. R. Jasperse, A. Kahan, J. N. Plendl, and S. S. Mitra, *Phys. Rev.* **146**, 526 (1966).
- ⁴⁰E. P. Wigner, *Phys. Rev.* **46**, 1002 (1934).
- ⁴¹M. J. L. Sangster and A. M. Stoneham, *Philos. Mag. B* **43**, 597 (1981).
- ⁴²G. Peckham, *Proc. Phys. Soc. London* **90**, 657 (1967).
- ⁴³W. C. Mackrodt, in *Computer Simulation of Solids*, edited by C. R. A. Catlow and W. C. Mackrodt (Springer-Verlag, Berlin, 1982), p. 175.
- ⁴⁴M. J. L. Sangster and D. K. Rowell, *Philos. Mag. A* **44**, 613 (1981).
- ⁴⁵M. Duclot and C. Departes, *J. Solid State Chem.* **31**, 377 (1980).
- ⁴⁶D. R. Sempolinski and W. D. Kingery, *J. Am. Ceram. Soc.* **63**, 664 (1980).
- ⁴⁷S. Shirasaki and M. Harma, *Chem. Phys. Lett.* **20**, 361 (1973).
- ⁴⁸S. Shirasaki and H. Yamamura, *Jpn. J. Appl. Phys.* **12**, 1654 (1970).
- ⁴⁹C. R. A. Catlow, R. James, W. C. Mackrodt, and R. F. Stewart, *Phys. Rev. B* **25**, 1006 (1982).
- ⁵⁰M. Leslie, *Solid State Ionics* **8**, 243 (1983).

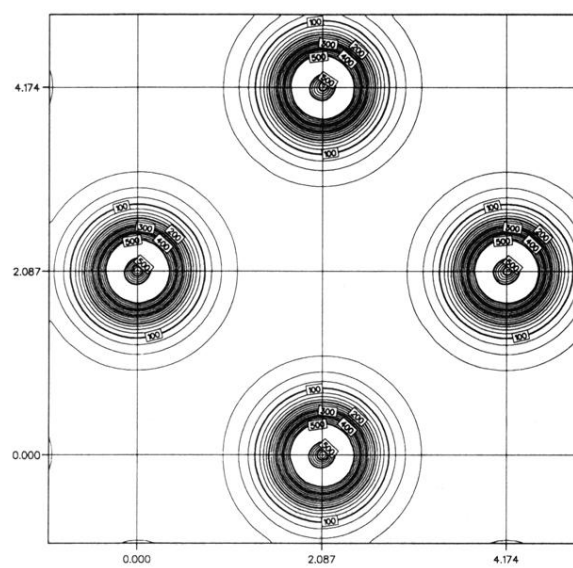


FIG. 2. Contour plot of the calculated valence electron density (units of 10^{-2} \AA^{-3}) on the (100) plane in perfect-crystal MgO. The contours are uniformly spaced at intervals of $25 \times 10^{-2} \text{ \AA}^{-3}$. Intersections of the grid lines mark regular-lattice sites. Distance along the edge of the plot is indicated in angstrom units.

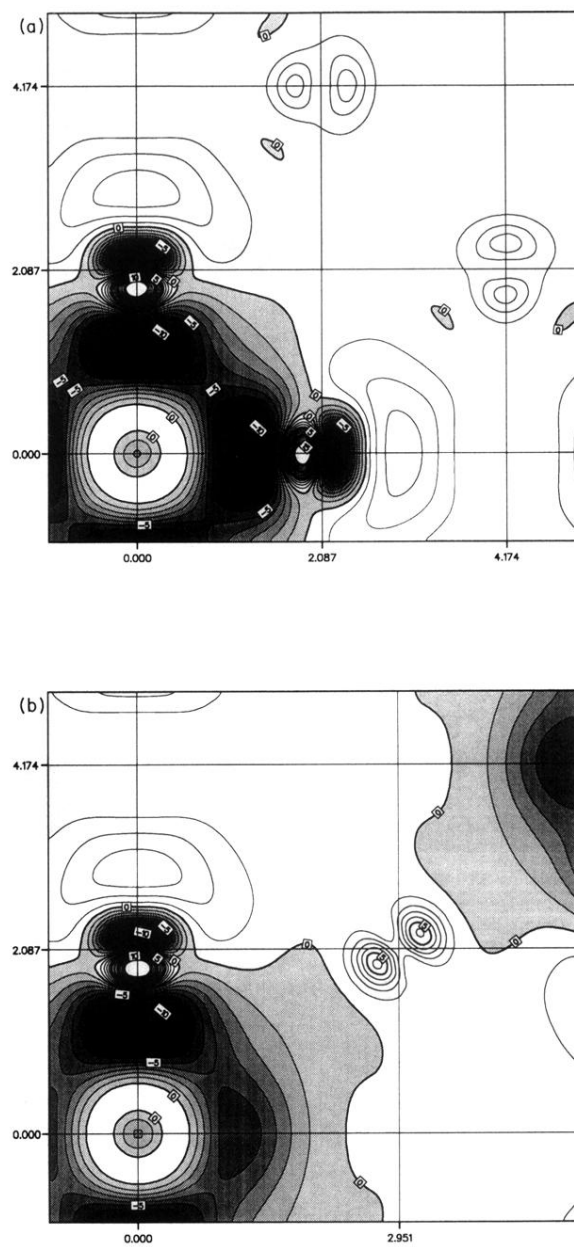


FIG. 3. Difference valence density (defective system minus perfect crystal) for the Mg^{2+} vacancy in MgO on (a) the (100) plane and (b) the (110) plane. Density is in units of 10^{-2} \AA^{-3} , with contours at intervals of 10^{-2} \AA^{-3} , and negative regions shown shaded. Intersections of the grid lines mark regular-lattice sites, with the vacancy site at the origin of coordinates. Distance along the edge of the plot is indicated in angstrom units.

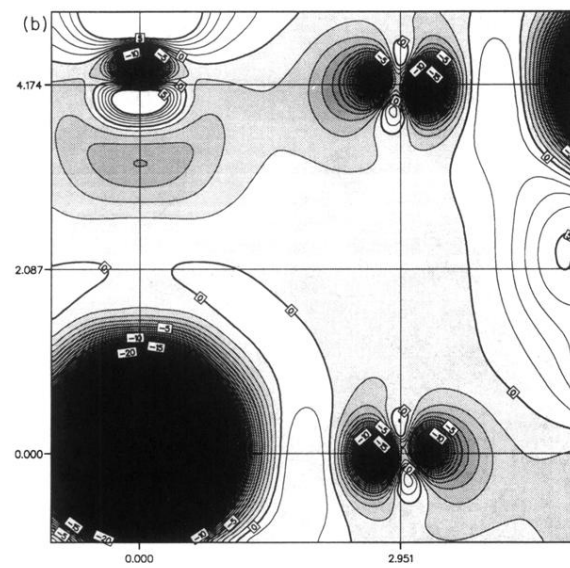
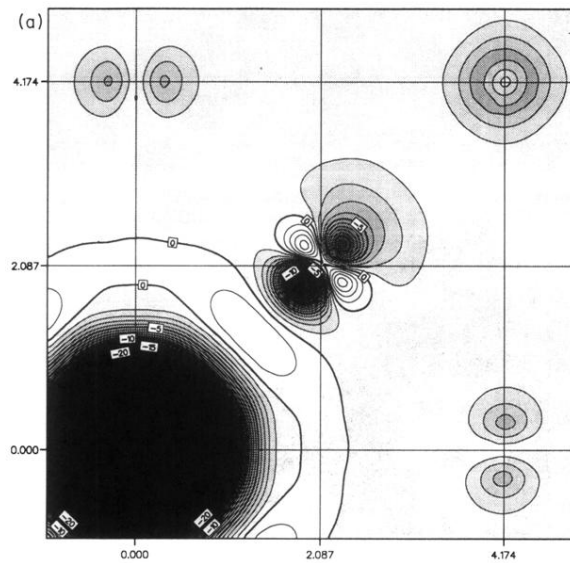


FIG. 4. Difference valence density (defective system minus perfect crystal) for the O^{2-} vacancy in MgO on (a) the (100) plane and (b) the (110) plane. Other details are the same as for Fig. 3.